Sperm exposure to carbon-based nanomaterials causes abnormalities in early development of purple sea urchin (*Paracentrotus lividus*)

Tina Mesarič[a], Kristina Sepčić[a], Damjana Drobne[a,b], Darko Makovec[b,c], Marco Faimali[d], Silvia Morgana[d], Carla Falugi[e], Chiara Gambardella[d]*

[a] Department of Biology, Biotechnical Faculty, University of Ljubljana, Slovenia

[b] Centre of Excellence in Nanoscience and Nanotechnology, Ljubljana, Slovenia

[c] Institute Jožef Stefan, Jamova 39, Ljubljana, Slovenia

[d] Institute of Marine Sciences, National Research Council, Genova, Italy

[e] Department of Environmental and Life Sciences, Università Politecnica delle Marche, Ancona, Italy

***Corresponding author: Chiara Gambardella**

ISMAR-CNR

Via de Marini 6

16149 Genova, Italy

Tel: +39-010-6475429

Fax: +39-010-6475400

E-mail: chiagamba@gmail.com, chiara.gambardella@ge.ismar.cnr.it

Abstract

We examined egg fertilisation in purple sea urchin (*Paracentrotus lividus*) after sperm exposure to carbon-based nanomaterials, carbon black (CB) and graphene oxide (GO), from 0.0001 mg/L to 1.0 mg/L. Gastrula stage embryos were investigated for acetylcholinesterase and propionylcholinesterase activities, and their morphological characteristics. Plutei were analysed for morphological abnormalities, with emphasis on skeletal rod formation. Egg fertilisation was significantly affected by CB, at all concentrations tested. Loss of cell adhesion at the gastrula surface was observed in eggs fertilised with sperm treated with CB. However, concentration-dependant morphological anomalies were observed in the gastrulae and plutei formed after sperm exposure to either CB or GO. The activities of both cholinesterases decreased in the gastrulae, although not in a concentration-dependent manner. These effects appear to arise from physical interactions between these carbon-based nanomaterials and the sperm, whereby nanomaterials attached to the sperm surface interfere with fertilisation, which leads to disturbances in the signalling pathways of early embryonic development. Reduced cholinesterase activity in gastrulae from eggs fertilised with nanomaterial-treated sperm confirms involvement of the cholinergic system in early sea urchin development, including skeletogenesis.

Keywords: acetylcholinesterase, carbon-based nanomaterials, development, propionylcholinesterase, sea urchin, sperm.

1. Introduction

Naturally occurring and industrially derived carbon-based nanomaterials are the most abundant nanomaterials in the environment (Hussain et al., 2009). Carbon black (CB) is a form of amorphous carbon that has extensive use in industrial applications (e.g., rubber products, paints, plastic, inks). CB is manufactured by controlled vapour-phase pyrolysis of hydrocarbons (CAS RN, 2013; Sorahan and Harrington, 2007), and it should not be confused with 'black carbon', which is a product of incomplete combustion of fossil fuels and biomass (Goldberg, 1985; Masiello and Druffel, 1998; Middleburg et al., 1999). Graphene oxide (GO) is formed of monomolecular sheets in which the carbon atoms are arranged in a graphene-like honeycomb lattice that is interrupted and terminated with numerous oxygen-containing functional groups (e.g., epoxy, carboxyl, hydroxyl). GO is an advanced and highly investigated nanomaterial that has physical and chemical characteristics that make it attractive for a variety of commercial and industrial purposes (Rao et al., 2009; Wang et al., 2011).

Due to the hydrophobic nature of carbon-based nanomaterials and their high surface-adsorption potential (Xia et al., 2011; Mesarič et al., 2013a), they can attach to different surfaces, including organisms, which might present a serious risk for biota (Klaine et al., 2008; Mesarič et al., 2013b). Although in recent years several ecotoxicological studies, on the impact of nanomaterials on marine organisms, have been performed (Canesi et al., 2008; Nielsen et al., 2008; Canesi et al., 2010a, 2010b; Rajasree et al., 2010; Miglietta et al., 2011; Carata et al., 2012; Falugi et al., 2012; Matranga et al., 2012; Miller et al., 2012; Ates et al., 2013; Mesarič et al., 2013b; Gambardella et al., 2014), there remains a lack of knowledge in this field.

The Mediterranean purple sea urchin (*Paracentrotus lividus*) is frequently used as a model in marine toxicology studies. **This species is widely diffused in benthic littoral zone of**

the Mediterranean and Atlantic (Boudouresque and Verlaque, 2001), an area that is strongly affected by human activities and pollution (ASTM, 2004). In these areas, *P. lividus* represents a key species, able to remodel hard bottoms and to cause barren grounds in *Posidonia* prairies by its grazing activity. Thus, this species is relevant for the control and organization of benthonic communities. While adult specimens are relatively resistant to pollution, the naked sperm and larval stages are directly affected by the presence of contaminants. Recently, it was reported that *P. lividus* planktonic larvae and benthonic adults can be affected by nanomaterials. Metal oxide nanomaterials (e.g, SnO_2, CeO_2, Fe_3O_4) have been found inside *P. lividus* immune cells after forced ingestion (Falugi et al., 2012). Furthermore, metal and metal oxide nanomaterials were reported to cause significant developmental anomalies in *P. lividus* embryos and larvae (Gambardella et al., 2013; Manzo et al., 2013). Similar data were reported by Manno et al. (2013) for carbon-based nanomaterials, which were shown to accelerate *P. lividus* embryonic development and induce embryonic malformations. In another study by the same group, carbon-based nanomaterials were reported to alter the expression of genes involved in biomineralisation (Manno et al., 2012). Carbon-based nanomaterials have also been shown to affect gene expression and development of sea urchin larvae, where they caused asymmetrical cell division and altered gene expression, again, with acceleration of development (Matranga et al., 2012). Gambardella et al. (2013) also provided evidence of altered embryonic development of sea urchins, along with effects of cholinergic signalling system in embryos, after fertilisation of eggs with sperm previously exposed to metal and metal oxide nanomaterials.

Neurotransmitters such as acetylcholine (ACh), biogenic amines, and γ-aminobutyric acid, are functionally active throughout ontogenesis (Buznikov et al., 1996). In particular, the cholinergic system is involved in both neuronal and non-neuronal signal transduction (Buznikov

et al., 1996), and its non-neuronal signalling function is best studied in processes of fertilisation and development in different animal species. Falugi et al. (1993) demonstrated the dependence of sperm motility on ACh receptors, and Baccetti et al. (1995) and Angelini et al. (2003) reported that sperm–egg fusion is based on signalling molecules of the cholinergic system. ACh availability and the correct functioning of both nicotinic and muscarinic ACh receptors, are responsible for ionic and cytoskeletal dynamics that are crucial for correct embryonic development of *P. lividus* (Aluigi et al., 2010; Falugi et al., 2008a; Falugi and Aluigi, 2012; Ravera et al., 2006). As ion channels gated by ACh, nicotinic receptors allow the inward passage of Na^+, while upon activation by ACh, muscarinic receptors trigger an intracellular transduction cascade that results in the release of Ca^{2+} from intracellular stores. It is expected that ACh receptor agonists and antagonists can either have direct effects on the ACh receptors, or have indirect effects, such as effects on the enzyme acetylcholinesterase (AChE), which degrades ACh. Thus, both ACh agonists and antagonists can affect the level of receptor activation, which can lead to alterations in signal transduction and cell-to-cell communication.

In the present study, we investigated fertilisation and early development of *P. lividus* when the eggs were fertilised with sperm that had been incubated in CB or GO suspensions. We assessed the following biomarkers for the effects of exposure of sperm to these carbon-based nanomaterials: (i) egg fertilisation; (ii) morphological features of embryos and larvae (i.e., gastrula and pluteus stages); and (iii) activities of two embryo (i.e., gastrula) cholinesterases: AChE (E.C. 3.1.1.7) and propionylcholinesterase (PChE; E.C. 3.1.1.8).

We expected here that these carbon-based nanomaterials will affect egg fertilisation by the previously exposed sperm, due to the high adsorption potential of these nanomaterials. Furthermore, these exposed sperm might transport the carbon-based nanomaterials to the eggs, where they can then interfere with fertilisation events. As the cholinergic system is involved in

regulation of the early embryonic developmental events in *P. lividus* (Angelini et al., 2003; Falugi et al., 2008a; Falugi and Aluigi, 2012), we hypothesised that any developmental anomalies would also be accompanied by altered cholinesterase activities in the developing embryos.

2. Materials and methods

2.1. Nanomaterials

The CB powder was from PlasmaChem GmbH (Germany). The mean size of the primary particles was ~20 nm (see Supplementary Information, **Fig. S1**). The GO was from Graphene Supermarket, as dry flakes with a mean size of 0.5 µm to 5.0 µm. At least 80% of the GO was of single-layer thickness, and according to the producer specification, the GO contained 20% by weight of oxygen. The CB and GO suspensions (final stock concentration, 1 mg/mL) were freshly prepared in 0.22-µm-filtered natural sea water (FNSW). The CB and GO stock suspensions were sonicated for 30 min in an ultrasonic bath (Falc sonicator, model LBS1; Italy), as described in Canesi et al. (2010a). **The assessment of the nanomaterial size of the CB and GO suspensions at a final concentration of 1 mg/mL by using dynamic light scattering was not possible as these nanomaterials strongly flocculate in FNSW (Mesarič et al., 2013b; Mesarič et al., 2015).** However, their characterisation in distilled water (Mesarič et al., 2013a) showed relatively high negative ζ-potentials (from -32 to -36 mV) for both of these nanomaterials. Furthermore, dynamic light scattering measurements of the CB suspension in distilled water showed substantial agglomeration of the particles, with sizes ranging from 60 nm to ~300 nm (Mesarič et al., 2013b). For the GO suspension in distilled water, analysis using dynamic light scattering was not possible because of the extremely anisotropic shapes of the primary particles (see Supplementary Information, **Fig. S2).** **The ξ-potential of nanomaterials**

suspended in the FNSW was determined to be much lower (around -14 mV) to that in the distilled water because of electrostatic screening effects related to the very high ionic strength (Mesarič et al., 2015).

Metals are used during nanomaterial synthesis, and the presence of metal ions (mainly Cu, Gd, Zn, Al and Fe) in nanomaterial leachates can induce significant toxicity in aquatic invertebrates and vertebrates. Thus, the presence of these metal ions should be considered when evaluating the toxicity of carbon-based nanomaterials (Hull et al., 2009). In line with this, FNSW suspensions of CB or GO used in tests described in this work, and also in experiments described in Mesarič et al. (2015), were analysed using energy-dispersive X-ray spectroscopy (EDS). These analyses revealed the absence of impurities in the form of metal ions. In both carbon-based nanomaterial suspensions in FNSW, also some evident cubic crystals were identified. Using EDS, they were confirmed to be composed of seawater salts (Fig. S3).

2.2. Egg fertilisation

Adult samples of *P. lividus* were collected along the coast of Genoa (Italy). They were transported to the laboratory in a refrigerated bag that was wrapped in towels that had been previously wet with sea water (Amemiya, 1996).

The spawning of the gametes was triggered by oral administration of 1‰ ACh in FNSW, with the eggs collected in standard FNSW. The sperm were collected directly from the genital pores and maintained in aliquots of 200 µL at 4 °C. The sperm from three different specimens were mixed. The experiments were repeated three times during the breeding season, with each carried out in triplicate. **Ten microliter aliquots of sperm suspensions were exposed to 1 mL CB or GO nanomaterial suspensions. Such a small volume of sperm was used since it has**

been demonstrated by contact with seawater within a brief period that the motility is initiated for almost 100% of sea urchin spermatozoa (Gibbons, 1981). CB and GO nanomaterial suspensions were prepared at the serial concentrations of: 0.0001, 0.001, 0.01, 0.1 and 1.0 mg/L, according to Gambardella et al. (2013, 2015). Since to date no regulatory guidelines are available for nanomaterials, the selected concentrations were chosen on the basis of those used for the reference toxicant (copper nitrate) for *P. lividus* spermiotoxicity test reported by the Italian guidelines (Arizzi Novelli et al., 2001, 2007a, b). No agglomerates of nanomaterials were observed under microscope in the FNSW, which is probably due to the short-term exposure period (1 h), as well as to low concentration of nanomaterials tested. Controls were performed by adding 10 µL standard FNSW instead of CB or GO nanomaterial suspensions. After 1 h of incubation of the sperm with the CB or GO nanomaterials, FNSW was added to each incubation mixture to a 1-mL final volume, and the suspensions **were centrifuged at 735 x *g* for 3 min at 4 °C (Mod. 5415 D, Eppendorf)**. **This experimental basis was used since at this speed sperm cells survive and are able to fertilize the eggs, whereas their motility could be affected at higher speed centrifugation forces (Tash et al., 2001).** The supernatants were discarded to remove the free nanomaterials, and the sediments (sperm with any bound nanomaterials) were resuspended in 1 mL FNSW. Ten microliters of these supernatants were then added to multiwell capsules containing 10 mL FNSW with approximately 300 eggs/mL. Under normal conditions, the egg activation occurred within 60 s of the sperm addition **(Alberts et al., 1989)**. To minimise the possibility of direct effects of the nanomaterials on the eggs and zygotes that might occur when the original protocol was used (Ghirardini et al., 2005), rinsing of the sperm was introduced before the fertilisation, as described above.

To determine the egg fertilisation in these incubations, 2 mL FNSW (containing approximately 600 fertilised and unfertilised eggs) was collected from each well 20 min after sperm addition, and fixed with 4% paraformaldehyde in FNSW for several hours. The eggs were then rinsed in physiological solution **(Tyrode, 1910).** The samples were observed under light microscopy (DM3000B, Leica, Germany) at 40× magnification, and the percentages of eggs showing a swollen perivitelline space, as the indication of fertilisation, were determined by counting under the microscope, from random fields with up to 600 eggs counted per treatment.

The reliability of the test was verified using the reference toxicant copper nitrate, according to Arizzi Novelli et al. (2002). The acceptability of the results was fixed at a fertilization rate > 70% in control tests (Arizzi Novelli et al., 2001; Volpi Ghirardini and Arizzi Novelli, 2001).

2.3. Analyses of embryotoxicity and skeletogenesis

The remaining 8 mL FNSW that contained ~2400 fertilised and unfertilised eggs (see section 2.2) were left to develop at 18 °C in a thermostatic room, and were sampled at 24, 48 and 72 h, which corresponded to the gastrula, early pluteus and pluteus stages, respectively. Unfertilised eggs and dead embryos were discarded 15 h after fertilisation.

For each sample, after 24, 48 and 72 h, approximately 100 larvae were fixed in cold methanol and 20% polyethylene glycol (Sigma, Italy). The developmental stages were monitored under light microscopy (DM3000B, Leica, Germany), including the formation of skeletal rods, and classified on the basis of morphology and synchronicity of development, as compared to the controls. This classification was according to the specific anomalies identified and recorded by Carballeira et al. (2012) and Gambardella et al. (2013). **The acceptability of the results was**

fixed at a percentage of normal development >70% in control tests (Arizzi Novelli et al., 2002).

2.4. Cholinesterase activity

The AChE and PChE activities were measured by the Ellman method (Ellman et al., 1961), modified for spectrophotometer use (6405 UV/VIS; Jenway). The 24 h old embryos at the gastrula stage were collected and maintained for 2 weeks at -20 °C. Prior to the AChE and PChE activity assays, these samples were homogenised, sonicated for 25 min in a bath sonicator (model LBS1; FALC, Italy), passed through a fine syringe needle (Ultrafin 29G, 12.7 mm length) in the presence of 1% Triton X100, **and centrifuged at 18,363 x *g*** for 30 s at 4 °C **(Mod. 5415 D, Eppendorf)**. The kinetics of the AChE and PChE activities were measured by following absorbance at 412 nm. The velocity of substrate cleavage was measured for 3 min, and compared with the linear equation of a standard curve that had been previously obtained by supplying known amounts of the cholinesterases. The protein content in the supernatants of the control and exposed gastrulae was measured by the Bradford method (Biorad, USA), and referred to a standard curve obtained with bovine serum albumin (Sigma, USA). The cholinesterase units were calculated as enzyme activity/min/mg protein. The measurements were performed in triplicate, using gastrulae from different parents, and were repeated three times during the reproductive season of *P. lividus*.

2.5. Statistical analysis

Statistical analysis of the cholinesterase activities for determination of significant differences between control and treated samples was performed using ANOVA (Bonferroni non-parametric *post-hoc* tests). A p value lower than 0.05 (p <0.05) was considered significant. The data are

presented as means ± standard error of three experiments, each of which was performed in triplicate. The significant differences among the treatments and concentrations are reported in the Figure legends.

3. Results

3.1. Egg fertilisation by sperm exposed to the carbon-based nanomaterials

The egg fertilisation by the *P. lividus* sperm was demonstrated by the cortical reaction of the egg that occurs in response to the first sperm–egg contact. This can be visualised by the elevation of the fertilisation layer and the appearance of the perivitelline space. The eggs showing this feature were considered as fertilised, and were counted. The counts under the different treatments were compared to the fertilisation of the control eggs, expressed as percentages. **In all experiments, controls showed 96 ± 3 % of fertilised eggs.** After the sperm were exposed to CB, the egg fertilisation was decreased by about 50% in comparison with the control, at all of the concentrations tested (0.0001-1.0 mg/L; **Fig. 1A**). In the case of the sperm exposed to GO, the egg fertilisation was not affected (**Fig. 1B).** **The repeatability of the experiments was tested by using copper nitrate as a reference toxicant. The test had a good repeatability, with an egg fertilisation decrease of about 50% at 0.01 mg/L (not shown), similar to previous results reported by Manzo et al. (2008).**

3.2. Morphological characteristics of gastrulae and plutei

The embryos sampled at the gastrula stage (24 h from fertilisation) that were obtained from eggs fertilised with *P. lividus* sperm that had been exposed to these carbon-based nanomaterials

showed anomalous and arrested development (**Fig. 2A-D**). The lowest concentration of CB (0.0001 mg/L) induced anomalous and arrested development in 3% of these embryos (**Fig. 2A**). The proportion of anomalous embryos greatly increased with exposure to the increasing concentrations of CB, and reached >80% at the highest concentration tested (1.0 mg/L; **Fig. 2A**). Following this CB exposure of the sperm, in the 72-h-old larvae at the pluteus stage, the anomalous plutei included developmentally delayed forms and those with skeletal damage (e.g., incomplete skeletal rods, crossed skeletal tips). These were seen in greater proportions than in the controls (**Fig. 2B**). Here, the highest proportions of anomalous larvae were seen at the lowest CB concentrations tested (87% and 80% at 0.0001 and 0.001 mg/L, respectively). At the highest CB concentration tested (1 mg/L), there was 54% anomalous larvae. GO induced a concentration-dependent increase in anomalies in the 24-h-old embryos (**Fig. 2C**). As for CB, non-developed embryos did not represent a significant percentage at any of the concentrations tested (1%-2%). The effects of GO on the development of the 72-h-old larvae was similar at all concentrations tested, with an overall mean of 70% ±10% anomalies, as compared to the control (**Fig. 2D**).

The morphology of the 24-h-old embryos at the gastrula stage obtained from the eggs fertilised with *P. lividus* sperm that had been exposed to these carbon-based nanomaterials is illustrated in Fig. 3 (upper panel). The embryos that developed from eggs fertilised with sperm exposed to the increasing concentrations of CB showed deterioration in their development. Anomalies in these embryos were observed at all of the CB concentrations tested, and were represented by irregular embryo shapes due to an anomalous migration of primary mesenchymal cells (Fig. 3a-f), by loss of cell-cell adhesion at the gastrula surface (Fig. 3c-f), as shown by the break-down of the epithelium in single separate cells (Fig. 3a-f), and by the lack of skeleton (Fig. 3 g). For the sperm exposure to GO (in the concentration range from 0.001 to 1 mg/L), the 24-h-old embryos also showed

anomalies (Fig. 3, lower panels). The main anomalies were represented by the break-down of the epithelium in single separate cells (Fig. 3b), by irregular embryo shapes (Fig. 3c-f), and by the incomplete skeletogenesis process (Fig. 3g).

Early pluteus larvae observed 48 h after fertilisation with *P. lividus* sperm that had been exposed to these carbon-based nanomaterials showed abnormalities in the skeletal architecture, and the larval shape and size, for both CB and GO exposure **at all tested concentrations** (**Fig. 4A**). This trend was also followed in the 72-h-old larvae at the pluteus stage, which showed time-dependent increases in the anomalies after egg fertilisation with the CB-exposed sperm, up to the point where their development was completely arrested. At 72 h, these larvae had the shape of the anomalous gastrula stage, they were smaller in size than the controls, and they lay at the bottom of the wells, without swimming (**Fig. 4B, f**). The 72-h-old larvae obtained from eggs fertilised with the GO-exposed sperm mainly showed anomalies in the skeletal architecture (e.g., lack of arms, crossed apex tips, arms not oriented to the mouth).

3.3. Cholinesterase activities

Significant differences were observed in the cholinesterase activities in the embryos after fertilisation with the *P. lividus* sperm that had been exposed to these carbon-based nanomaterials. The AChE activities were significantly lowered in 24-h-old embryos obtained after the sperm had been exposed to either CB or GO, at all of the concentrations tested (**Fig. 5A, B**). The sperm exposure to CB induced an overall mean of 35% inhibition of the AChE activity (**Fig. 5A**), and a similar overall mean inhibition of 40% after the sperm exposure to GO (**Fig. 5B**). This inhibition of the AChE activity was not dose-dependent. A similar trend was observed for the PChE activity (**Fig. 5C, D**). In the embryos obtained from the sperm exposed to CB, the inhibition of the PChE activity was also not dose-dependent, and showed an overall mean inhibition of 75% compared to

the control, across all of the concentrations tested (**Fig. 5C**). PChE activity was also inhibited in the embryos that developed from the eggs fertilised with the sperm exposed to GO; however, at the GO concentration of 0.001 mg/L, there was an increase in the enzyme activity (**Fig. 5D**).

4. Discussion

4.1. Egg fertilisation by sperm exposed to CB and GO

The data from the present study indicate that the *P. lividus* sperm exposure test appears to be very sensitive to **carbon-based nanomaterials, such as CB and GO**. Here, exposure of the sperm to even the lowest concentration of CB tested (0.0001 mg/L) induced adverse effects, while exposure of the *P. lividus* embryos themselves to the same type of nanomaterial at 66 mg/L was previously reported to be non-embryotoxic (Miglietta et al., 2011). **It was shown previously that sea urchin sperm cells are more sensitive to toxic compounds than the embryos (Manzo et al., 2008). Male gametes are released naked into the seawater, exposing their membrane receptors directly to the environment and therefore also to the contaminants (Falugi and Prestipino, 1987), including nanomaterials. Conversely, embryos are surrounded by a fertilisation envelope, that makes them more resistant to different environmental factors (Giudice, 1973).**

Sperm cells can be affected by different substances in a direct manner, with reduction or suppression of egg fertilisation, and/or indirectly, where transmission of damage to the offspring occurs. In the present study, we observed both types of effects in the case of the exposure of the *P. lividus* sperm to CB, but only indirect effects when the sperm were exposed to GO. **We believe that physical interactions, such as attachment of the carbon-based nanomaterials to**

the sperm surface, will be one of the main reasons for the observed decrease in egg fertilisation by these sperm that is caused by CB. It should be considered that the process of low-speed and short-term centrifugation, that was used here to separate the free nanomaterials from the sperm-bound nanomaterials (Chapter 2.2), might have also enhanced the attachment of nanomaterials to the sperm surface. However, in such a case one would expect that the fertilization ability of sperm exposed to GO, which forms much larger particles than CB, would be also considerably affected.

The adsorption potential of nanomaterials has already been suggested as being responsible for their biological effects. For example, ZnO-induced sperm toxicity and embryotoxicity in *P. lividus* was reported to be related not only to the zinc ions, but also to surface interactions of particle/ aggregates with the target cells/ organisms (Manzo et al., 2013). Similarly, CB has been reported to attach to sperm of the alga *Fucus serratus*, thus removing the sperm from the suspension, which significantly affected the egg fertilisation by these sperm (Nielsen et al., 2008).

These reports and the data from the present study are in line with the study of Xia et al. (2011), who calculated the surface adsorption indices for different groups of nanomaterials, and reported that carbon-based nanomaterials have considerably higher adsorption potential compared to metal-based nanomaterials. These differences in adsorption potential appear to be responsible for the observed lower adverse effects of metal and metal-based nanomaterials (Gambardella et al., 2013), in comparison to the carbon-based nanomaterials investigated in the present study under the same experimental set-up. Also, these data show different behaviours of the two carbon-based nanomaterials tested, in terms of egg fertilisation by the exposed sea urchin sperm: the exposure to GO did not affect the egg fertilisation, while the exposure to CB significantly decreased it.

These different behaviours can be explained by the different characteristics of these two carbon-based nanomaterials, such as their sizes, shapes, and surface adsorption potentials. **Although similar ζ-potentials of the GO and CB suspensions were measured in FNSW (Mesarič et al., 2015),** these two nanomaterials show different inherent hydrophilicities. CB is inherently relatively hydrophobic; however, it adsorbs charged species (ions and charged molecules) onto its surface from the liquid medium. On the contrary, GO has a hydrophilic character due to its oxygen-containing functional groups (e.g., epoxy, carboxyl, hydroxyl). Xia et al. (2011) also showed that pure carbon-based nanomaterials like CB show much greater surface adsorption potential than polar carbon nanomaterials like GO. We believe that these properties of CB allow stronger adsorption of this nanomaterial to the sperm cells, resulting in higher level of disturbances during the egg fertilization process.

4.2. Early developmental alterations

4.2.1. Inhibition of cholinesterase activity in embryos

We found significant, but not dose-dependent, inhibition of the activities of both of the enzymes investigated, as AChE and PChE, in gastrulae obtained after egg fertilisation with sperm exposed to both CB and GO. **Considering that ACh is absent in sea urchin sperm up to the fertilization process, this molecule, as well as its related enzymes (Angelini et al., 2004; Falugi et al., 2008b), were not measured in the sperm in the present study. We measured the AChE activity only in the embryos, since this enzyme plays multiple roles during embryonic development (e.g. it is involved in cell-to-cell communication (Falugi and Aluigi, 2012), modulation of apoptosis (Zhang et al., 2002) and driving morphogenetic movements (Drews, 1975) independently from the cholinergic system.**

As also reported previously (Falugi and Aluigi, 2012; Gambardella et al., 2013), greater effects were seen here on the PChE activity. However, when sperm were exposed to metal (Ag, Co; (Gambardella et al., 2013)) or metal oxide (TiO_2; Gambardella, personal communication) nanomaterials, these effects were not as large as in the present study with the same experimental set-up. Gambardella et al. (2013) reported both increased and decreased AChE and PChE activities in *P. lividus* embryos.

The cholinergic system is active in the acrosome, neck region, and flagellum of the sea urchin sperm (Falugi et al., 2008a), as well as in the eggs (Angelini et al., 2003), where it has an important role in the fertilisation process (Falugi et al., 2008a). We believe that when these carbon-based nanomaterials become attached to the sperm surface, they will affect ACh release from the sperm **during the fertilization process**, possibly by inhibition of the membrane-exposed choline acetyltransferase, or even through inhibition of the nicotinic ACh receptors or AChE at the surface of the oocyte during fertilisation. This will lead to anomalous influx of Na^{2+}, and will thus affect membrane depolarisation. These events can lead to altered ACh synthesis through choline acetyltransferase in fertilised eggs, and will subsequently alter the expression of muscarinic receptors (Harrison et al., 2002). It is these muscarinic receptors that are responsible for modulation of the intracellular concentrations of Ca^{2+}, which is a major second messenger that provides key activating signals in non-parthenogenic development, through cell-to-cell communication, cell-cycle control, protein (including cholinesterases) synthesis, and cell locomotion (Wilding et al., 1996; Kashir et al., 2013). Consequently, the specific activities of the cholinesterases in the embryos that show developmental anomalies differ from those in the controls.

4.2.2. Alterations in embryonic and larval morphology

As discussed in the previous section, any disturbances to the process of fertilisation can result in the loss of downstream signal transduction, which can lead to altered intracellular ion concentrations, including Ca^{2+} (Van Koppen and Kaiser, 2003). As reported by Ravera et al. (2006) and Falugi et al. (2008a), ionic dynamics are crucial for correct cell migration during gastrulation and embryonic development of sea urchins. This process is again ultimately dependent on ACh availability.

Our data here show that egg fertilisation with the CB-exposed sperm influences cell-cell adhesion during gastrulation, which includes altered directional migration and ingression of primary mesenchymal cells (Malinda et al., 1994; Miller et al., 1997). Gambardella et al. (2013) did not observe these changes in a same experimental set-up where the sperm were exposed to Ag, Co or TiO_2 nanomaterials. Again, we believe that the lower adsorption potential of the nanomaterials investigated by Gambardella et al. (2013) resulted in their lower adsorption onto the sperm cells, and consequently in lower levels of disturbance during egg fertilisation and the early developmental events.

Furthermore, we show here that the exposure of sea urchin sperm to both of the carbon-based nanomaterials tested results in anomalous arrangements of the skeletal rods. These effects were even more pronounced at the developmental stages of plutei (48 h, 72 h, after fertilisation), and they might also be a consequence of impaired primary mesenchymal cell migration, which is responsible for larval skeletogenesis (**Peterson and McClay, 2003;** Bradham et al., 2004; Kominami and Takata, 2004; Gambardella et al., 2015). Altered skeletogenesis as a common response to environmental stress, and this was also reported after exposure of sea urchin gametes (Pesando et al., 2003; Gambardella et al., 2013) and early embryos (Carballeira et al., 2012; Siller et al., 2013) to other environmental contaminants. On the other hand, Manno et al. (2012) reported altered biomineralisation processes due to carbon nanoparticle exposure of pluteus

larvae, through the activation of one of the genes controlling skeletogenesis. They explained that the larvae activate a defence process against the external material by incorporation of the nanoparticles into microstructures of aragonite, similar to pearl oysters.

Previous studies (Angelini et al., 2003; Ravera et al., 2006; Falugi et al., 2008a; Aluigi et al., 2010) have reported that ACh availability is ultimately important for ionic dynamics, and consequently for correct cell migration during gastrulation and embryonic development in sea urchins. The data from the present study also show reduced activities of the cholinesterases. This thus provides experimental confirmation that developmental anomalies are accompanied by alterations in the activity of the cholinergic system, and it can be used as a reliable and sensitive biomarker of developmental anomalies.

5. Conclusions

Here we have described the consequences of exposure of *P. lividus* sperm to the carbon-based nanomaterials CB and GO, in terms of the egg fertilisation and early developmental stages of the purple sea urchin (i.e., gastrulae, plutei).

We have confirmed the more severe effects of CB on egg fertilisation by these sperm, while the exposure to GO had no effects on egg fertilisation up to a sperm-exposure concentration of 1 mg/L. However, embryos and larvae obtained after egg fertilisation with the *P. lividus* sperm exposed to either of these carbon-based nanomaterials showed similar morphological effects and inhibition of the activities of the enzymes tested: AChE and PChE. We believe that these effects are a consequence of the attachment of these carbon-based nanomaterials to the surface of the sperm, and their consequent interactions with fertilisation events. Carbon-based nanomaterials can disrupt the cholinergic system of the gamete cell surface, which will lead to alterations in the signalling pathways involved in early embryonic development. In particular, sperm exposure to

very low amounts of these carbon-based nanomaterials can provoke these above-described effects on the developmental stages of *P. lividus*. **To date no environmental concentration in seawater is available either in bibliography or in official databases for CB or GO. Anyway, the predicted environmental concentration reported for other substances such as benzo[a]pyrene (CAS No 50-32-8), involved in carbon black production process, is about 0.015 µg/L (https://www.env.go.jp/en/chemi/chemicals/profile_esrac/profile5/pf1-22.pdf), representing a lower concentration than those tested in the present study.** However, it is worth noting that the reported environmental concentrations of CB in polluted freshwaters (as 0.08 µg/mL to 7.5 µg/mL, CAS RN, 2013), correspond to the concentrations that are shown to have toxic effects on sea urchins in the present study. **In conclusion, we can speculate that the adverse effects of carbon-based NMs on sperm and embryos of the sea urchin might occur also on other shallow water species, in particular those forming the benthonic communities, where the more or less agglomerated nanomaterials sink and accumulate.**

Acknowledgments

The authors would like to gratefully acknowledge RITMARE Flagship Project, a National Research Programme funded by the Italian Ministry of University and Research (MIUR) and the Slovene Human Resources Development and Scholarship Fund, for financial support, of Tina Mesarič. A special thank to Dr. Christopher Berrie for reading and critical appraisal of the manuscript.

References

Alberts, B., Bray, D., Lewis, J., Raff, M., Roberts, K., Watson, J.D. 1989. Molecular biology of the cell. Garland Publishing, New York.

Aluigi, M.G., Falugi, C., Mugno, M.G., Privitera, D., Chiantore, M. 2010. Dose-dependent effects of chlorpyriphos, an organophosphate pesticide, on metamorphosis of the sea urchin, *Paracentrotus lividus*. Ecotoxicology 19, 520-529.

Amemiya, S. 1996. Complete regulation of development throughout metamorphosis of sea urchin embryos devoid of macromeres. Dev. Growth Differ. 38, 465-476.

American Society for Testing Materials (ASTM). 2004. Standard guide for conducting static acute toxicity tests with embryos of echinoid embryos. E1563-E1598.

Angelini, C., Amaroli, A., Falugi, C., Di Bella, G., Matranga, V. 2003. Acetylcholinesterase activity is affected by stress conditions in *Paracentrotus lividus* coelomocytes. Mar. Biol. 143, 623-628.

Angelini, C., Baccetti, B., Piomboni, P., Trombino, S., Aluigi, M.G., Stringara, S., Gallus, L., Falugi, C. 2004. Acetylcholine synthesis and possible functions during sea urchin development. Eur. J. Histochem. 49, 235-244.

Arizzi Novelli, A., Volpi Ghirardini, A., Ghetti, P.F. 2001. Sperm cell and embryotoixcity test with *Paracentrotus lividus* LMK. Reproducibility and comparison of sensitivity with other echinoid species using copper. Biol. Mar. Medit. 8.

Arizzi Novelli, A., Argese, E., Tagliapietra, D., Bettiol, C., Volpi Ghirardini, A., 2002. Toxicity of tributylin and triphenyltil to early life-stages of *Paracentrotus lividus* (Echinodermata: Echinoidea). Environ. Toxicol. Chem. 21, 859-864.

Arizzi Novelli, A., Losso C., Falugi C., Giuliani S., Kozinkova L., Lera S., Leoni T., Manzo S., Mazziotti C., Pellegrini D., Picone M., Volpi Ghirardini, A. 2007 a. Il test di

fecondazione con il riccio di mare *Paracentrotus lividus* (LMK) Biol. Mar. Medit. 14, 43-47.

Arizzi Novelli, A., Losso C., Volpi Ghirardini A., Ghetti, P.F. 2007 b. Saggi di tossicita' con il riccio di mare *Paracentrotus lividus*: percorso di validazione di metodologie per gli ambienti di transizione attraverso una procedura di controllo qualità. Biol. Mar. Medit. 14:100-102.

ASTM (American Society for Testing, Materials), 2004. Standard guide for conducting static acute toxicity tests with embryos of echinoid embryos. E1563–E1598.

Ates, M., Daniels, J., Arslan, Z., Farah, O.I., Rivera, H.F. 2013. Comparative evaluation of impact of Zn and ZnO nanoparticles on brine shrimp (*Artemia salina*) larvae: effects of particle size and solubility on toxicity. Environ. Sci. Processes Impacts 15, 225.

Baccetti, B., Burrini, A.G., Collodel, G., Falugi, C., Moretti, E., Piomboni, P. 1995. Localization of two classes of acetylcholine receptor-like molecules in sperms of different animal species. Zygote 3, 207-217.

Boudouresque, C.F., Verlaque, M., 2001. Ecology of *Paracentrotus lividus*. In: Lawrence, J.M. (Ed.) Edible sea urchins: biology and ecology 32. Elsevier Science, Amsterdam 177-216.

Bradham, C.A., Miranda, E.L., McClay, D.R. 2004. PI3K inhibitors block skeletogenesis but not patterning in sea urchin embryos. Dev. Dynam. 229, 713-721.

Buznikov, G.A., Shmukler, Y.B., Lauder, H.M. 1996. From oocyte to neuron: do neurotransmitters function in the same way through development? Cell. Mol. Neurobiol. 16, 533-559.

Canesi, L., Ciacci, C., Betti, M., Fabbri, R., Canonico, B., Fantinati, A., Marcomini, A., Pojana, G. 2008. Immunotoxicity of carbon black nanoparticles to blue mussel hemocytes. Environ. Int. 34, 1114-1119.

Canesi, L., Ciacci, C., Vallotto, D., Gallo, G., Marcomini, A., Pojana, G. 2010a. *In-vitro* effects of suspensions of selected nanoparticles (C60 fullerene, TiO_2, SiO_2) on *Mytilus* hemocytes. Aquat. Toxicol. 96, 151-158.

Canesi, L., Fabbri R., Gallo, G., Vallotto, D. 2010b. Biomarkers in *Mytilus galloprovincialis* exposed to suspensions of selected nanoparticles (Nano carbon black, C-60 fullerene, nano-TiO_2, nano-SiO_2). Aquat. Toxicol. 100, 168-177.

Carata, E., Tenuzzo, B.A., Arnò, F., Buccolieri, A., Serra, A., Manno, D., Dini, L. 2012. Stress response induced by carbon nanoparticles in *Paracentrotus lividus*. Int. J. Mol. Cell. Med. 1, 30-38.

Carballeira, C., Ramos-Gómez, J., Martín-Díaz, L., DelValls, T.A. 2012. Identification of specific malformations of sea urchin larvae for toxicity assessment: application to marine pisciculture effluents. Mar. Environ. Res. 77, 12-22.

CAS RN 2013, Screening assessment for the challenge: Carbon Black. 2013. Chemical Abstracts Service Registry: 1333-86-4.

Drews, U., 1975. Cholinesterase in embryonic development. Prog. Histochem. Cytochem. 7, 1-52.

Ellman, G.L., Courtney, K.D., Andres, V.J., Featherstone R.M. 1961. A new rapid colorimetric determination of acetylcholinesterase activity. Biochem. Pharmacol. 7, 88-95.

Falugi, C., Prestipino, G., 1987. Effects of some inhibitors of the cholinegic system, active during the sea urchin *Paracentrotus lividus* development. In: Boudoresque, C.F. (Ed.),

Colloque International sur *Paracentrotus lividus*. Gis Posidonie, Marseille, France, pp. 147-155.

Falugi, C., Pieroni, M., Moretti, E. 1993. Cholinergic molecules and sperm functions. J. Submicr. Cytol. Path. 25, 63-69.

Falugi, C., Lammerding-Koppel, M., Aluigi, M.G. 2008a. Sea urchin development: an alternative model for mechanistic understanding of neurodevelopment and neurotoxicity. Birth Defects Embryo Res. C Embryo Today 84, 188-203.

Falugi, C., Collodel, G., Moretti, E., Piomboni, P., Aluigi, M.G., Angelini, C., Baccetti, B., 2008b. A neural-like model for sperm-egg interactions. Involvement of the cholinergic system. In: Collodel, G., Moretti, E. (Eds), Sperm Morphology and Pathology, 2008: 000-000 ISBN: 978-81-308-0280-0.

Falugi, C., Aluigi, M.G., Chiantore, M.C., Privitera, D., Ramoino, P., Gatti, M.A., Fabrizi, A., Pinsino, A., Matranga, V. 2012. Toxicity of metal oxide nanoparticles in immune cells of the sea urchin. Mar. Environ. Res. 76, 114-121.

Falugi, C., Aluigi, M.G. 2012. Early appearance and possible functions of non-neuromuscular cholinesterase activities. Front. Mol. Neurosci. 5, 1-12.

Gambardella, C., Aluigi, G. M., Ferrando, S., Gallus, L., Ramoino, P., Gatti, A.M., Rottigni, M., Falugi, C. 2013. Developmental abnormalities and changes in cholinesterase activity in sea urchin embryos and larvae from sperm exposed to engineered nanoparticles. Aquat. Toxicol. 130-131, 77-85.

Gambardella, C., Mesarič, T., Milivojević, T., Sepčić, K., Gallus, L., Carbone, S., Ferrando, S., Faimali, M. 2014. Effects of selected metal oxide nanoparticles on *Artemia salina* larvae: evaluation of mortality and behavioural and biochemical responses. Environ. Monit. Assess. 186, 4249-4259.

Gambardella, C., Ferrando, S., Morgana, S., Gallus, L., Ramoino, P., Ravera, S., Bramini, M., Diaspro A., Faimali M., Falugi C. 2015. Exposure of *Paracentrotus lividus* male gametes to engineered nanoparticles affects skeletal biomineralization and larval plasticity. Aquat. Toxicol., 158, 181-191.

Ghirardini, A.V., Novelli, A.A., Losso, C., Ghetti, P.E. 2005. Sperm cell and embryo toxicity tests using the sea urchin *Paracentrotus lividus* (LmK). Techniq. Aquat. Toxicol. 8, 2.

Gibbons, I.R., 1981. Cilia and flagella of eukaryotes. J. Cell Biol. 91, 107s-124s.

Giudice, G., 1973. Developmental biology of the sea urchin embryo. Academic Press, USA. pp. 469.

Goldberg, E.D. Black Carbon in the Environment: Properties and Distribution. John Wiley & Sons, New York (1985) 198.

Harrison, P.K., Falugi, C., Angelini, C., Whitaker, M. 2002. Muscarinic signalling affects intracellular calcium concentration during the first cell cycle of sea urchin embryos. Cell Calcium 31, 289-297.

Hull, M.S., Kennedy, A.J., Steevens, J.A., Bednar, A.J., Weiss, J.C.A., Vikesland, P.J. 2009. Release of metal impurities from carbon nanomaterials influences aquatic toxicity. Environ. Sci. Technol. 43, 4169-4174.

Hussain, S., Boland, S., Baeza-Squiban, A., Hamel, R., Thomassen, C.L., Martens, A.J., Billon-Galland, M.A., Fleury-Feith, J., Mosain, F., Pairon, J.C., Marano, F. 2009. Oxidative stress and proinflammatory effects of carbon black and titanium dioxide nanoparticles: role of particle surface area and internalized amount. Toxicology 260, 142-149.

Kashir, J., Deguchi, R., Jones, C., Coward, K., Stricker, S.A. 2013. Comparative biology of sperm factors and fertilization-induced calcium signals across the animal kingdom. Mol. Reprod. Dev. 80, 787-815.

Klaine, S.J., Alvarez, P.J., Batley, G.E., Fernandes, T.F., Handy, R.D., Lyon, D.Y., Mahendra, S., McLaughlin, M.J., Lead, J.R. 2008. Nanomaterials in the environment: behaviour, fate, bioavailability and effects. Environ. Toxicol. Chem. 27, 1825-1851.

Kominami, T., Takata, H. 2004. Gastrulation in the sea urchin embryo: a model system for analysing the morphogenesis of a monolayered epithelium. Dev. Growth Differ. 46, 309-326.

Malinda, K.M., Ettensohn, C.A. 1994. Primary mesenchyme cell migration in the sea urchin embryo: distribution of directional cues. Dev. Biol. 164, 562-578.

Manno, D., Carata, E., Tenuzzo, B., Panzarini, E., Buccolieri, A., Filippo, A., Rossi, M., Serra, A., Dini, L. 2012. High ordered biomineralization induced by carbon nanoparticles in the sea urchin *Paracentrotus lividus*. Nanotechnology 23, 495104.

Manno, D., Serra, A., Buccolieri, A., Panzarini, E., Carata, E., Tenuzzo, B., Izzo, D., Vergallo, C., Rossi, M., Dini, L. 2013. Silver and carbon nanoparticles toxicity in sea urchin *Paracentrotus lividus* embryos. BioNanoMaterials 14, 229-238.

Manzo, S., Buono, S., Cremisini, C. 2008. Predictability of copper, irgarol, and diuron combined effects on sea urchin *Paracentrotus lividus*. Arch. Environ. Contam. Toxicol. 54, 57-68.

Manzo, S., Miglietta, M.L., Rametta, G., Buono, S., Di Francia, G. 2013. Embriotoxicity and spermiotoxicity of nanosized ZnO for Mediterranean sea urchin *Paracentrotus lividus*. J. Hazard. Mater. 254-255, 1-9.

Masiello, C.A., Druffel, E.R.M. 1998. Black carbon in deep-sea sediments. Science 280, 1911-1913.

Matranga, V., Corsi, I. 2012. Toxic effects of engineered nanoparticles in the marine environment: model organism and molecular approaches. Mar. Environ. Res. 76, 32-40.

Mesarič, T., Baweja, L., Drašler, B., Drobne, D., Makovec, D., Dušak, P., Dhawan, A., Sepčić, K. 2013a. Effects of surface curvature and surface characteristics of carbon-based nanomaterials on the adsorption and activity of acetylcholinesterase. Carbon 62, 222-232.

Mesarič, T., Sepčić, K., Piazza, V., Gambardella, C., Garaventa, F., Drobne, D., Faimali, M. 2013b. Effects of nano carbon black and single-layer graphene oxide on settlement, survival and swimming behaviour of *Amphibalanus amphitrite* larvae. Chem. Ecol. 29, 643-652.

Mesarič, T., Gambardella, C., Milivojević, T., Faimali, M., Drobne, D., Falugi, C., Makovec, D., Jemec, A., Sepčić, K. 2015. High surface adsorption properties of carbon-based nanomaterials are responsible for mortality, swimming inhibition, and biochemical responses in *Artemia salina* larvae. J. Aquat. Toxicol., in press. doi:10.1016/j.aquatox.2015.03.014

Middleburg, J.J., Nieuwenhuize, J., Can Breuge, P. 1999. Black carbon in marine sediments. Mar. Chem. 65, 245-252.

Miglietta, M.L., Rametta, G., Francia, G.D., Manzo, S., Rocco, A., Carotenuto, R., Picione, L.D.F., Buono, S. 2011. Characterization of nanoparticles in seawater for toxicity assessment towards aquatic organisms. Sensor. Microsy. 91, 425-429.

Miller, J.R., McClay, D.R. 1997. Characterization of the role of cadherin in regulating cell adhesion during sea urchin development. Dev. Biol. 15, 323-339.

Miller, R.J., Bennett, S., Keller, A.A., Pease, S., Lenihan, H.S. 2012. TiO_2 nanoparticles are phototoxic to marine phytoplankton, PLoS ONE 7, e30321.

Ministry of the Environment, Government of Japan, Profiles of the Initial Environmental Risk Assessment of Chemicals, Vol. 5, https://www.env.go.jp/en/chemi/chemicals/profile_esrac/profile5/pf1-22.pdf, accessed 26.3.2015.

Nielsen, H.D., Berry, L.S., Stone, V., Burridge, T.R., Fernandes, F. 2008. Interactions between carbon black nanoparticles and the brown algae *Fucus serratus*: inhibition of fertilization and zygotic development. Nanotoxicology 2, 88-97.

Peterson, R.E., McClay, D.R. 2003. Primary mesenchyme cell patterning during the early stages following ingression. Dev. Biol. 254, 68-78.

Pesando, D., Huitorel, P., Dolcini, V., Angelini, C., Guidetti, P., Falugi, C. 2003. Biological targets of neurotoxic pesticides analysed by alteration of developmental events in the Mediterranean sea urchin, *Paracentrotus lividus*. Mar. Environ. Res. 55, 39-57.

Rajasree, R.S.R., Vumar, G.V., Abraham, S.L., Indabakandan, D. 2010. Studies on the toxicological effects of engineered nanoparticles in environment – a review, Int. J. Appl. Bioengineer. 4, 2.

Rao, C.N.R., Biswas, K.S., Subrahmanyam, K.S., Govindaraj, A. 2009. Graphene, the new carbon. J. Mater. Chem. 19, 2457-2469.

Ravera, S., Falugi, C., Calzia, D., Pepe, I.M., Panfoli, I., Morelli, A. 2006. First cell cycles of sea urchin *Paracentrotus lividus* are dramatically impaired by exposure to extremely low-frequency electromagnetic field. Biol. Reprod. 75, 948-953.

Siller L., Lemloh M.L., Piticharoenphun S., Mendis B.G., Horrocks B.R., Brümmer F., Medaković D. 2013. Silver nanoparticle toxicity in sea urchin *Paracentrotus lividus*. Environ. Pollut. 178, 498-502.

Sorahan, T., Harrington, J.M. 2007. A "lugged" analysis of lung cancer risks in UK carbon black production workers, 1951-2004. Amer. J. Ind. Med. 50, 555-564.

Tash, J.S., Kim, S., Schuber, M., Seibt, D., Kinsey, W.H. 2001. Fertilization of sea urchin eggs and sperm motility are negatively impacted under low hypergravitational forces significant to space flight. Biol. Reprod. 65, 1224-1231.

Tyrode, M.V. 1910. The mode of action of some purgative salts. Arch. Int. Pharmacodyn. 20, 205.

Van Koppen, C.J., Kaiser, B. 2003. Regulation of muscarinic acetylcholine receptor signalling. Pharmacol. Ther. 98, 197-220.

Volpi Ghirardini, A., Arizzi Novelli A. 2002. A cell sperm toxicity test procedure for the Mediterranean species *Paracentrotus lividus* LMK (Echinodermata: echinoidea). Environ. Technol. 22, 439-445.

Wilding, M., Wright, E.M., Patel, R., Ellis-Davies, G., Whitaker, M. 1996. Local perinuclear calcium signals associated with mitosis entry in early sea urchin embryos. J. Cell Biol. 135, 191-199.

Wang, Y., Li, Z., Wang, J., Li, J., Lin, Y. 2011. Graphene and graphene oxide: biofunctionalization and applications in biotechnology. Trends Biotechnol. 29, 205-212.

Xia, X.R., Monteiro-Riviere, N.A., Mathur, S., Song, X., Xiao, L., Oldenberg, S.J., Fadeel, B., Riviere, J.E. 2011. Mapping the surface adsorption forces of nanomaterials in biological systems, ACS Nano. 5, 9074-9081.

Zhang, X.J., Yang, L., Zhao, Q., Caen, J.P., He, H.Y., Jin, Q.H., Guo, L.H., Alemany, M., Zhang, L.Y., Shi, Y.F. 2002. Induction of acetyl-cholinesterase expression during apoptosis in various cell types. Cell Death Diff. 9, 790-800.

Figure legends:

Figure 1. Egg fertilisation by the *P. lividus* sperm exposed for 1 h to CB **(A)** and GO **(B)**, according to the exposure concentrations, as compared to the controls (0). Data are means ±standard error of three independent experiments.

Figure 2. **Larval development** anomalies and their classification following egg fertilisation by the *P. lividus* sperm exposed for 1 h to CB **(A, B)** and GO **(C, D)**, according to the 24-h-old gastrulae (**A, C**) and 72-h-old plutei (**B, D**) and the exposure concentrations, as compared to the controls (0). ND, non-developed gastrulae or arrested development; AD, anomalous development; D, normal development; del, delayed forms; sk, skeletal anomalies. Data are means ±standard error of three independent experiments.

Figure 3. Representative morphological features of embryos 24 h after egg fertilisation (gastrula stage) by the *P. lividus* sperm exposed to CB or GO (as indicated). Black asterisks, anomalous migration of primary mesenchymal cells; white asterisks, loss of cell-cell adhesion; arrow, absence of skeleton in gastrula; arrowheads, gastrulae with irregular shapes. Scale bars: 50 µm.

Figure 4. Representative morphological features of embryos 48 h **(A)** and 72 h **(B)** after egg fertilisation (pluteus stages) by the *P. lividus* sperm exposed to CB or GO (as indicated). Asterisks, incomplete or erroneous migration of skeleton elements; arrows, anomalous arrangement of skeletal rods (crossed tips). Scale bar: 50 µm.

Figure 5. Acetylcholinesterase (A,B) and propionylcholinesterase activity (C, D) in 24 h old *P. lividus* embryos obtained after egg fertilisation with sperm exposed to either carbon black (A,C) or graphene oxide (B,D). Data, representing the mean value ± SE (n = 3), were analysed by ANOVA followed by Bonferroni *post hoc* test. * $p<0.05$. CB, carbon black; GO, graphene oxide.

Supporting Information

Transmission electron microscopy of the nanomaterials

For the transmission electron microscopy investigations, the nanomaterials were deposited by the drying of the aqueous suspension on copper-grid-supported, perforated, transparent carbon foil. The transmission electron microscopy analysis was performed using a JEOL 2010 F electron microscope, operated at 200 kV. The carbon black (CB) is seen as agglomerates of amorphous, globular primary nanoparticles, with sizes of ~20 nm (**Figure S1**). For the graphene oxide (GO), according to the data from the producer, at least 80% of this is in the form of 0.5-μm to 5-μm-wide sheet-like molecules. However, when the aqueous GO suspension was dried on the transmission electron microscopy support, the GO deposited on the in the form of plate-like aggregates of different thicknesses. **Figure S2** shows the edge of a thin platelet aggregate lying on the perforated, amorphous-carbon-support layer. The different contrast in the image shows buckling and folding of the GO layers.

Supplementary Figure legends

Figure S1. Representative transmission electron microscopy image of CB.

Figure S2. Representative transmission electron microscopy image of GO.

Figure S3. Energy-dispersive X-ray spectroscopy (EDS) analysis of carbon-based nanomaterials suspended in FNSW: (A) only FSNW suspensions without NM; (B) carbon

black in FNSW, and (C) graphene oxide in FNSW. EDS spectra shown on the right correspond to position marked with white arrows. All results in tables are in weight %.

Figure(s)

Click here to download high resolution image

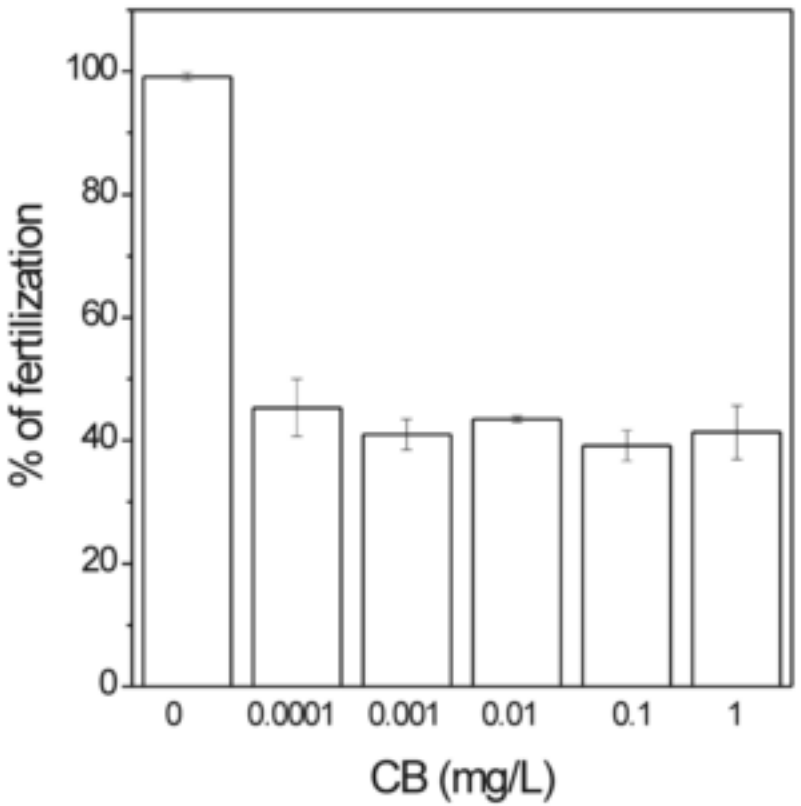

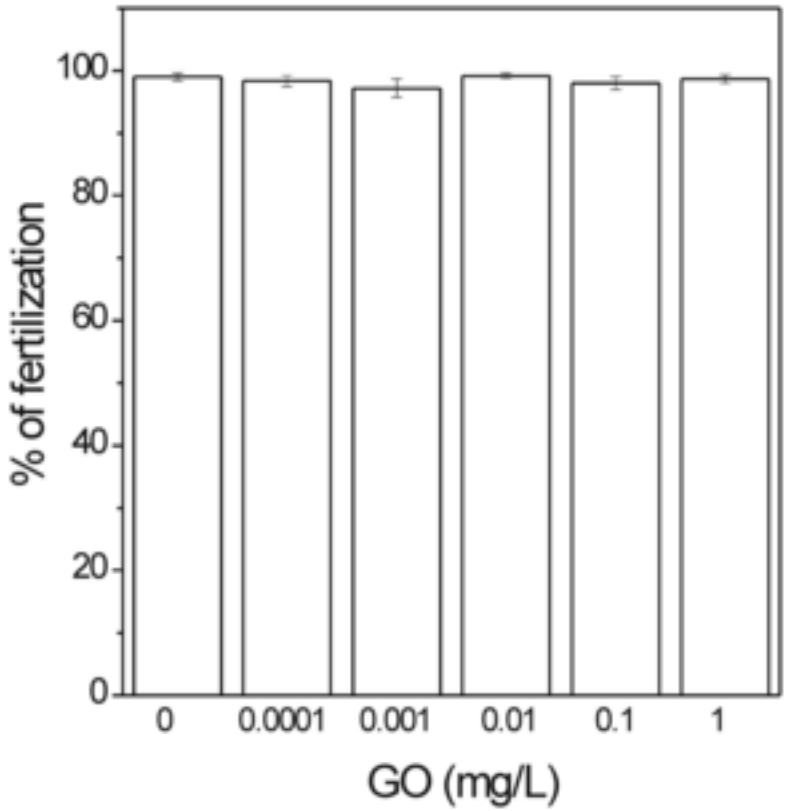

Figure(s)

Click here to download high resolution image

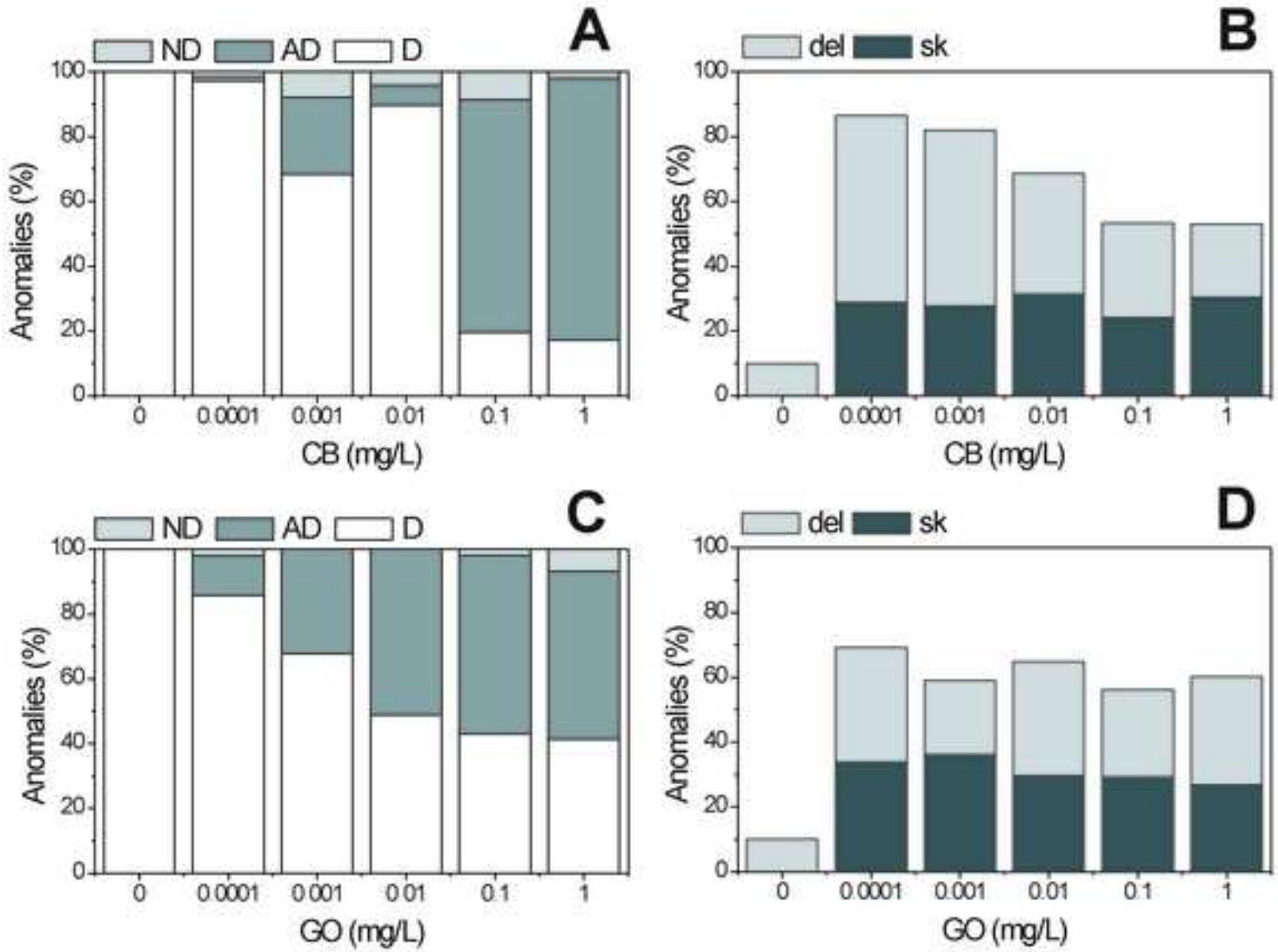

Figure(s)

Click here to download high resolution image

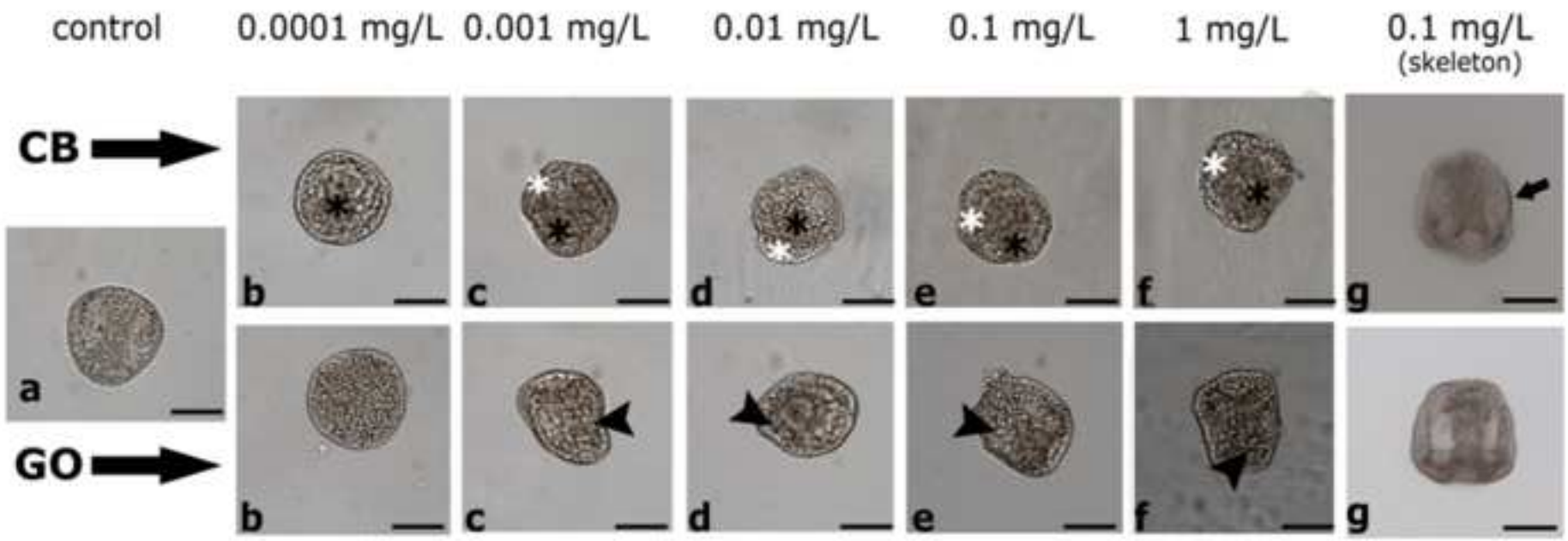

Figure(s)

Click here to download high resolution image

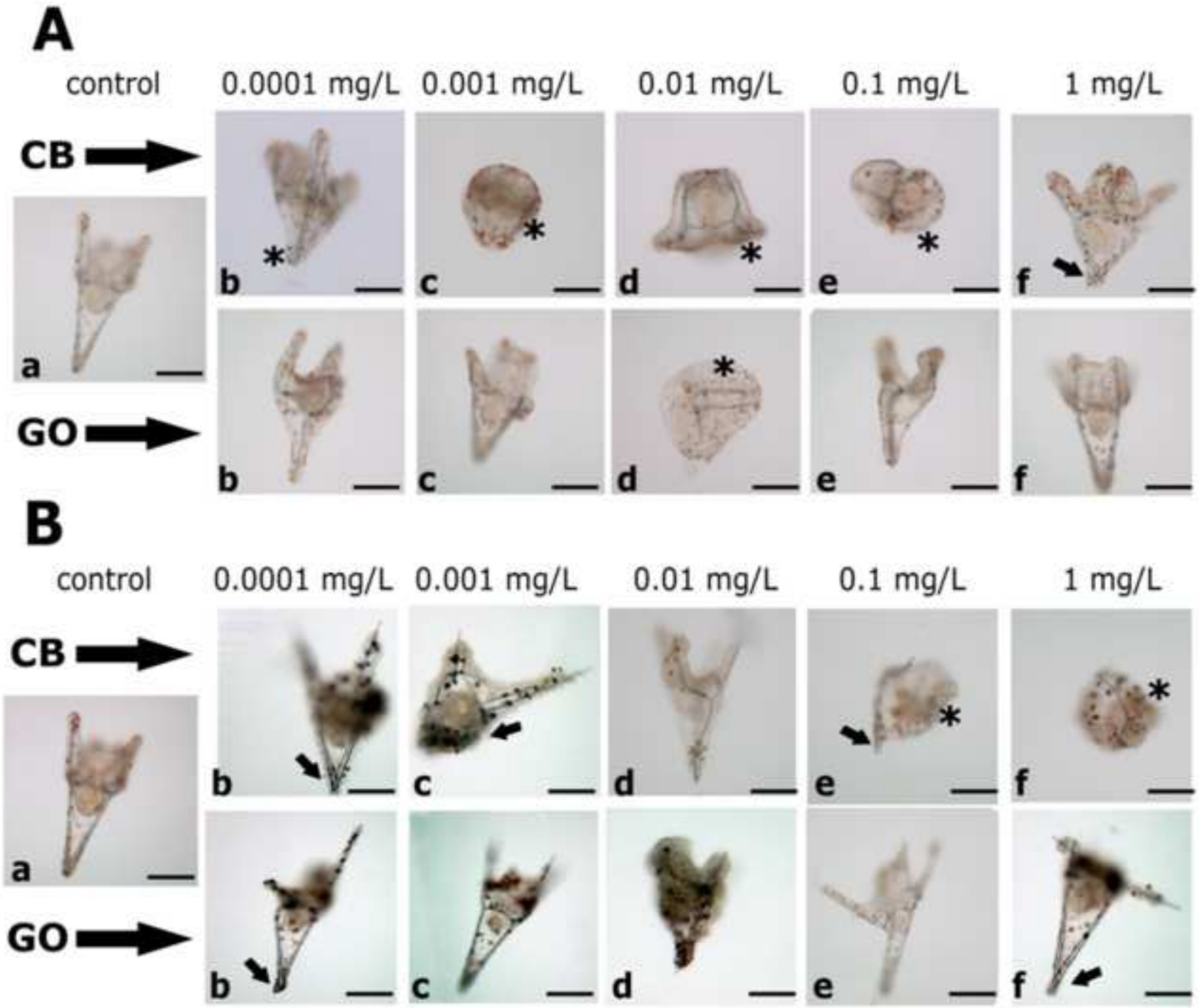

Figure(s)

Click here to download high resolution image

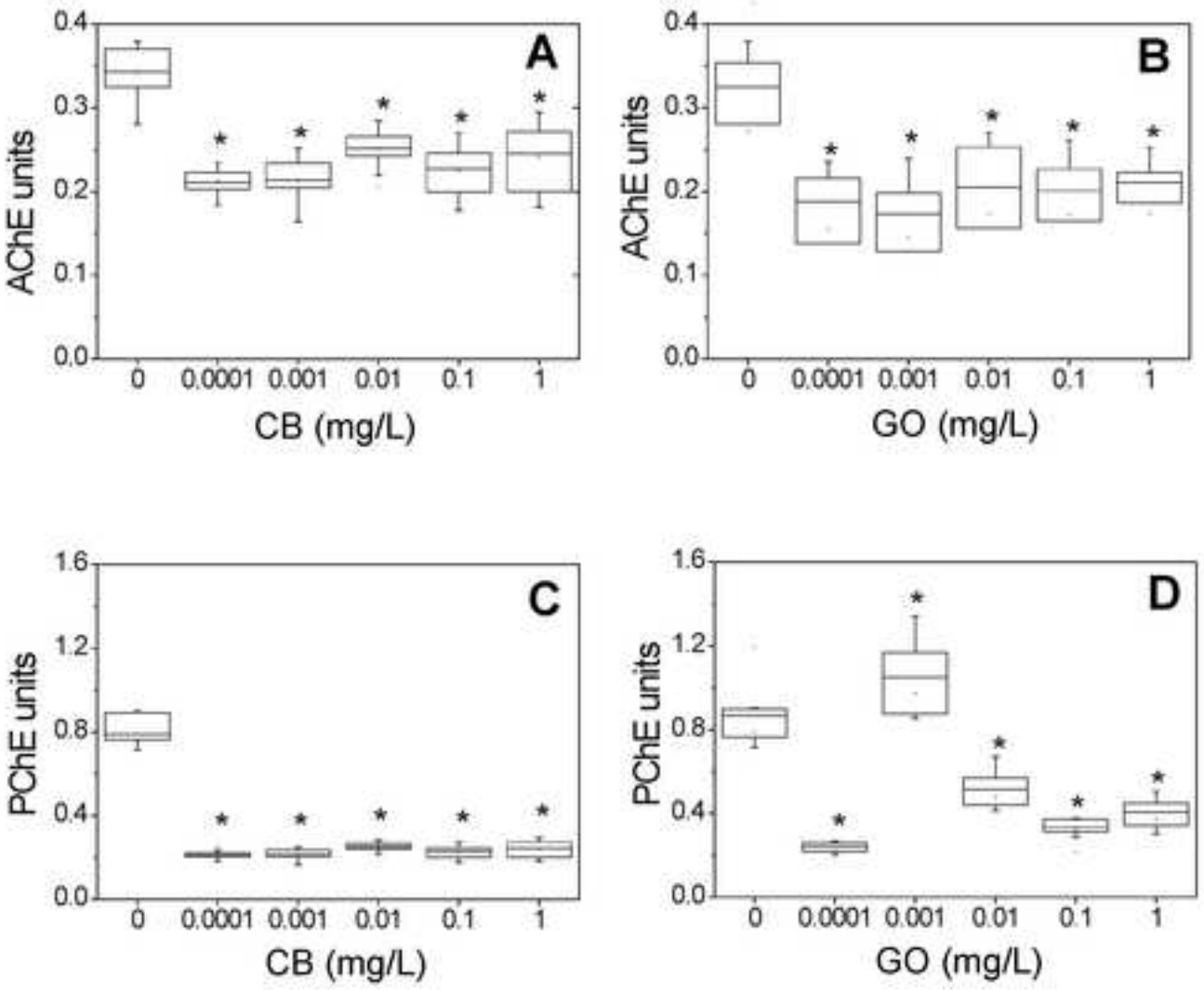

Supplementary Material

Click here to download Supplementary Material: Mesari et al. Figure S1.tif

Supplementary Material

Click here to download Supplementary Material: Mesari et al. Figure S2.tif

Supplementary Material

Click here to download Supplementary Material: Mesaric et al. Figure S3.docx

Highlights:

- CB exposure of *P. lividus* sperm reduces egg fertilisation already at 0.0001 mg/L
- GO exposure of *P. lividus* sperm does not affect egg fertilisation at up to 1 mg/L
- CB and GO exposure of sperm induce developmental anomalies in gastrulae and plutei
- CB and GO exposure of sperm reduce cholinesterase activities in gastrulae